

# Microsurgical Creation of Giant Bifurcation Aneurysms in Rabbits for the Evaluation of Endovascular Devices

Branko Popadic<sup>1,2,3</sup>, Florian Scheichel<sup>1,2,3</sup>, Cornelia Pangratz-Daller<sup>1,2,3</sup>, Roberto Plasenzotti<sup>4</sup>, Camillo Sherif<sup>1,2,3</sup>

<sup>1</sup> Karl Landsteiner University of Health Sciences <sup>2</sup> Department of Neurosurgery, University Hospital St. Pölten <sup>3</sup> Cerebrovascular Research Group, Department of Neurosurgery, University Hospital St. Pölten <sup>4</sup> Division of Biomedical Research, Medical University of Vienna

## Corresponding Author

Camillo Sherif

camillo.sherif@stpoelten.lknoe.at

## Citation

Popadic, B., Scheichel, F., Pangratz-Daller, C., Plasenzotti, R., Sherif, C. Microsurgical Creation of Giant Bifurcation Aneurysms in Rabbits for the Evaluation of Endovascular Devices. *J. Vis. Exp.* (199), e63738, doi:10.3791/63738 (2023).

## Date Published

September 8, 2023

## DOI

10.3791/63738

## URL

jove.com/video/63738

## Introduction

Endovascular embolization has become an important alternative to aneurysm clipping for the treatment of ruptured cerebral aneurysms<sup>1</sup>. The main drawback of this treatment strategy is the high rates of aneurysm recanalization with delayed aneurysm rupture<sup>2</sup>. Large and giant aneurysms have been shown to be especially prone to these complications. Therefore, new endovascular devices are constantly being

developed<sup>3</sup>. Models for experimental studies are essential for testing these devices<sup>4,5</sup>.

Human cerebral aneurysms have been studied in rats, rabbits, canines, and swine<sup>6,7,8</sup>. However, rabbit models have shown the best comparability to humans regarding hemodynamics and the coagulation system<sup>9,10,11,12</sup>. In the venous pouch arterial bifurcation model in rabbits, a venous pouch is sutured into a microsurgically created

## Abstract

Giant aneurysms are dangerous lesions requiring endovascular treatment, with high rates of aneurysm recanalization and re-rupture. Reliable *in vivo* models are rare but are required for testing new endovascular devices. We demonstrate the technical aspects of the creation of giant bifurcation aneurysms in New Zealand white rabbits (2.5-5.5 kg). A 25-30 mm long venous pouch is taken from the external jugular vein, and a bifurcation between both carotid arteries is created microsurgically. The pouch is sutured in the bifurcation to mimic a giant aneurysm. This protocol summarizes our previously published standard technique for venous pouch true arterial bifurcation aneurysms and highlights its essential modification steps for giant aneurysms. Using this modified technique, we were able to create an animal model for giant aneurysms with high comparability to humans regarding the hemodynamics and coagulation systems. Furthermore, low morbidity and high aneurysm patency rates were achieved. The proposed giant aneurysm model offers an excellent possibility for testing new endovascular devices.

true bifurcation of both common carotid arteries (CCA) to mimic an aneurysm<sup>13</sup>. However, a true bifurcation model for giant aneurysms in rabbits was not available until recently. The first results using computational fluid dynamics and biomechanical testing were published by our group in 2016<sup>14</sup>.

As giant aneurysms represent challenging lesions for treatment in humans and a reliable animal model is crucial for their research, we present a condensed summary of the improved techniques for the creation of giant experimental aneurysms<sup>12,13</sup>. The advantages of using this method are (i) the minimal morbidity and high aneurysm patency rates<sup>14</sup>, high comparability to humans regarding hemodynamics and the coagulation system<sup>9,10,11,12</sup>, and cost-effectiveness compared to canine methods, (ii) the true bifurcation design for a giant aneurysm<sup>13</sup>, (iii) the good hemodynamic comparability of the created aneurysms shown by computational fluid dynamics<sup>14</sup>, and (iv) the high long-term patency rates<sup>15</sup>.

## Protocol

The animal studies were approved by the Institute Animal Ethics Committee of the institute at which this study was conducted. For this animal model, New Zealand white rabbits (2.5-5.5 kg) were used.

**NOTE:** Our standard technique for the creation of the venous pouch true arterial bifurcation aneurysms in rabbits was published in 2011, and an adaption for giant aneurysms was published in 2016<sup>12,13</sup>. We summarize these techniques and highlight essential steps for the modification of giant aneurysms.

### 1. Preoperative phase

1. Administer ketamine (30 mg/kg) and xylazine (6 mg/kg) *via* perilumbar intramuscular injection for general anesthesia. Then, intubate the rabbit (tube diameter: 4 mm, length: 18 mm; this size may vary depending on the animal's size), and continue with gas anesthesia (2% isoflurane). Monitor the depth of anesthesia by a toe pinch every 15 min, and adjust if necessary.
2. Shave the area from the angle of the jaw down to the thorax using clippers. Disinfect the surgical area using at least three alternating rounds of chlorhexidine or povidone-iodine scrub followed by alcohol. Drape the surgical site.

### 2. Surgical phase I

1. Incise the skin along the midline from the angle of the jaw down to the manubrium sterni using a scalpel. Perform blunt dissection in the subcutis.
2. Switch to the surgical microscope. Dissect a 2-3 cm long branchless segment of the left external jugular vein. Apply 4% papaverine dropwise repeatedly on the vessels to prevent vasospasm and optionally add 5 mg/mL neomycin sulfate dropwise for infection control.
3. Harvest the vein segment after proximal and distal ligation using 6-0 non-resorbable sutures. Put the vein segment in a heparinized saline solution (1,000 IU heparin in 20 mL of 0.9% saline and 1 mL of 4% papaverine HCl)<sup>13</sup>.

### 3. Surgical phase II

1. Prepare both CCAs by dissecting them from the carotid bifurcation down to their origin. Watch carefully for the

medial arterial branches, which supply the laryngeal, tracheal, and neural structures.

2. Administer 1,000 IU heparin intravenously.
3. Apply a temporal microsurgical clip at the distal end of the right CCA.
4. Ligate and cut the right CCA proximally directly above the brachiocephalic trunk using poly filament 6-0 non-resorbable sutures.
5. Use a sterile piece of rubber (e.g. from a glove) as an underlay to facilitate the procedure. Remove the adventitia at the anastomosis site of both vessels with anatomic micro-forceps and micro-scissors. Clip the anastomosis site of the left CCA distally and proximally<sup>13</sup>.

#### 4. Surgical phase III

1. Make an arteriotomy at the left CCA according to the size of the planned anastomosis with the right CCA and the venous pouch. Determine the length of the arteriotomy by the diameter of the contralateral carotid artery (about 2 mm) together with the size of the planned aneurysm neck.  
**NOTE:** The size is as flexible as the possible aneurysm sizes and neck sizes of this universal aneurysm model. The minimum size should not be smaller than 3 mm and can be up to a maximum of about 15 mm.
2. Clean the aneurysm site with heparinized saline (about 5 mL). Using four to five non-resorbable 10-0 monofilament sutures, and suture the posterior circumference of the right CCA stump with the before-described arteriotomy of the left CCA.
3. Cut the stump of the right CCA longitudinally to a length of 1-1.5 cm. Anastomose the posterior part of the venous

pouch with the arteriotomy of the left CCA using 10-0 sutures. Then, suture the rear side of the venous pouch with the posterior wall of the right CCA with three to four sutures.

4. Suture the anterior anastomosis in the same sequence.
5. Release the temporal clip on the right CCA. Usually, the anastomosis leaks. Use this to wash air and blood clots out.
6. Seal the anastomosis with fat derived from the subcutaneous tissue of the surgical approach and fibrin glue.
7. Close the fascia using 4-0 non-resorbable sutures. Perform the wound closure using 4-0 resorbable sutures<sup>13</sup>.

#### 5. Postoperative phase

1. Administer 10 mg/kg acetylsalicylic acid intravenously.
2. Achieve postoperative analgesia by a transdermal fentanyl patch (12.5. µg/h) at the shaved region for 3 days<sup>13</sup>.  
**NOTE:** Consult the facility veterinarian on appropriate analgesia options.
3. Achieve postoperative anticoagulation by administering 100 IU/kg low molecular heparin daily subcutaneously for 2 weeks.

#### Representative Results

In 2011, we published an improved technique for the venous pouch arterial bifurcation model for the creation of aneurysms in rabbits<sup>16</sup>. The mean aneurysm length was 7.9 mm, and the mean neck width was 4.1 mm. By using interrupted suture and aggressive anticoagulation, we were able to achieve 0%

mortality and patency in 14 of 16 aneurysms. This technique was then adapted for the creation of giant aneurysms, and computational fluid dynamics and biomechanical testing were performed in 2016<sup>14</sup>. In this study, the anesthesiologic management was also changed from the use of ventilation masks to intubation due to the availability of an experienced veterinarian. This represents a critical step in our experience, as the intubation of a rabbit can be difficult and lead to high preoperative mortality rates. Furthermore, the postoperative

anticoagulation with low molecular heparin was reduced from 250 IU/kg to 100 IU/kg. With this regime, we were able to achieve 0% mortality and patency in 11 of 12 aneurysms. The aneurysm lengths were 21.5-25.6 mm, with neck widths from 7.3-9.8 mm. Detailed results of this study are shown in **Table 1**. Furthermore, these aneurysms were used for the evaluation of endovascular devices. An image of a stent-assisted embolized giant aneurysm after aneurysm retrieval is shown in **Figure 1**.

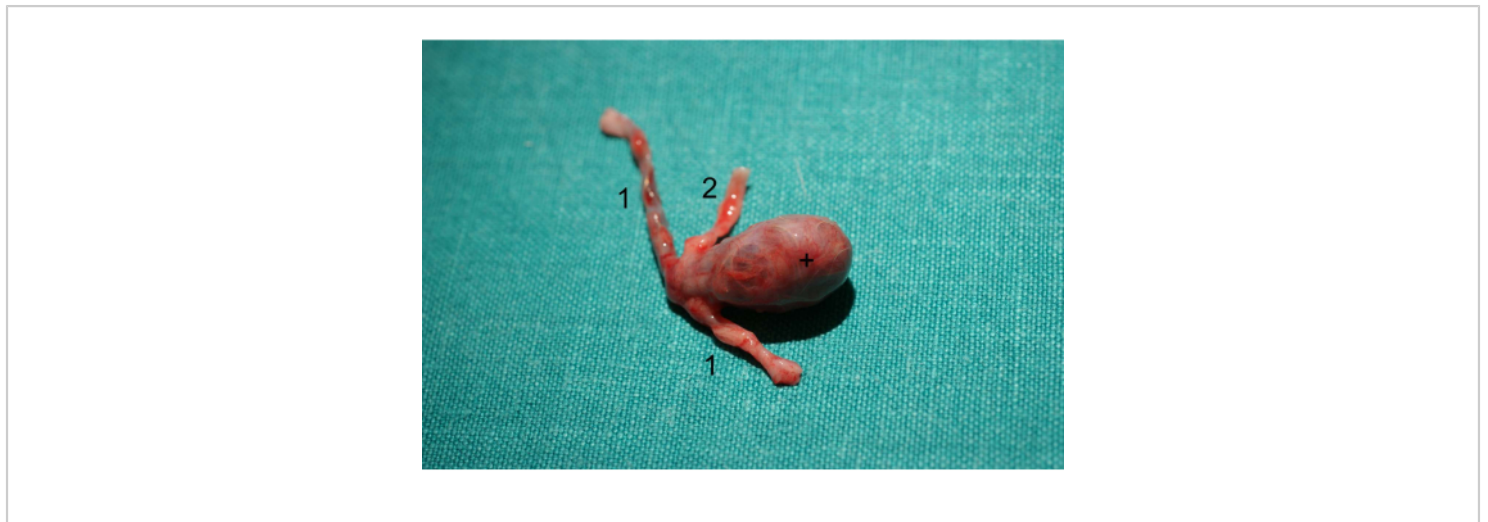


**Figure 1: Photo of a stent-assisted embolized giant aneurysm after aneurysm retrieval.** 1 left CCA, stented parent vessels; 2 right CCA, parent vessel; + embolized aneurysm sac. [Please click here to view a larger version of this figure.](#)

Aneurysm No.	Patency	Parent artery diameter [mm]	Length [mm]	Neck width [mm]	Dome width [mm]	Aspect-ratio [-]
2	no	--	--	--	--	--
1	yes	2.4	23.4	7.7	9.9	3
3	yes	2.2	25.1	8.7	10.3	2.9
4	yes	2.5	23.5	9.8	10.6	2.4
5	yes	2.8	24.8	8.6	9.8	2.9
6	yes	2.5	21.5	9.8	9.3	2.2
7	yes	2.2	24.2	7.9	10.5	3.1
8	yes	2.3	25.6	9.3	10.2	2.8
9	yes	2.4	22.1	7.3	10	3
10	yes	2.2	25.6	8.9	9.7	2.9
11	yes	2.3	23.4	9.7	11.1	2.4

**Table 1: Aneurysm data generated for computational fluid dynamics and biomechanical testing.** The updated and detailed results of 11 aneurysms created in 2016 are shown. This table has been modified from Sherif et al.<sup>14</sup>.

## Discussion

There are some critical steps to ensure the replicability of the protocol described above. The meticulous removal of the thrombogenic periadventitial tissue at the anastomosis site is essential<sup>13</sup>. One must ensure that the anastomosis is tensionless and has as few sutures as possible. For giant aneurysms, it is important to begin with the back side of the anastomosis. This gives better sight and control for the most challenging sutures as compared to previously proposed procedures<sup>17, 18, 19</sup>.

Contrary to normal-sized aneurysms, the key factor for the retrieval of the venous pouch is the meticulous preparation of a 2-3 cm long vein segment. It is crucial to dissect all the small side branches of the external jugular vein to be able to safely

ligate them. While suturing the anastomoses, direct contact with the vessels should be avoided by leaving the ends of the single sutures a bit longer. Only these free suture ends should be grabbed with the forceps to move the aneurysm complex. This technical detail helps in the use of a no-touch technique with the vessels, which is a general principle in vascular microsurgery. Another challenge, as compared to normal-sized aneurysms, is the impaired sight to the back side of the vessel aneurysm complex caused by the giant aneurysm sac. This can lead to increased technical difficulties at the rear side of the anastomosis. After completing the anastomosis, a longer flushing time is necessary due to the higher thrombus formation probability within the giant aneurysm sac. One should be aware of leakages, as they are very common. If

they are not sealed with the fat pad, additional sutures should be performed.

A limitation is the use of an extracranial aneurysm as a model for intracranial pathology. Furthermore, high microsurgical requirements and well-equipped laboratories are needed for the successful implementation of this protocol. Also, rabbits are sensitive animals, and good animal housing is crucial for survival rates.

The presented model offers several advantages over the current widely used models. The most widespread current model for cerebral aneurysms is the elastase model. However, for this model, biomechanical testing of the aneurysm wall properties has never been performed. Therefore, the biomechanical comparability of this model to human conditions is unclear. On the contrary, this biomechanical testing is available for our proposed model, showing good comparability to human conditions<sup>14</sup>. Another significant advantage of this proposed model over the elastase model is the true bifurcational hemodynamics<sup>18</sup>. This model is created in a true artificially created bifurcation, while the elastase-digested aneurysm sac is formed at the dead end of the CCA, more or less mimicking a sidewall geometry.

Up to this date, there were nearly no other giant aneurysm models available. However, these models are strongly needed for the evaluation of new endovascular devices. Going through the literature, only one canine model for giant bifurcation aneurysms has been described<sup>20</sup>. However, canine hemodynamics and the coagulation system showed significant differences in comparison to humans, whereas the rabbit model has shown its superiority regarding its comparability to humans<sup>14</sup>.

Newly developed endovascular devices for aneurysm treatment are commonly tested in rabbit models. Our previously published venous pouch bifurcation aneurysms model has been used for the CE and FDA approval of such devices<sup>3,18</sup>. However, a reliable and comparable animal model for giant aneurysms in rabbits was not available until recently. In humans, giant aneurysms have the highest rates of recanalization and delayed rupture after endovascular treatment. Therefore, new endovascular devices are urgently wanted, and the industry has brought up the need for a giant aneurysm rabbit model. Another application is the evaluation of the aneurysm wall using high-field magnetic resonance imaging, which aims to identify potential risk factors for rupture, such as aneurysm wall diameter or contrast enhancement behavior<sup>22</sup>. Furthermore, long-term studies are needed to evaluate the patency of this aneurysm model over time, as well as studies showing the aneurysm behavior with flow diverter stents and intrasaccular flow diverters.

## Disclosures

The authors have no relevant financial or non-financial interests to disclose.

## Acknowledgments

We are grateful to Professor Heber Ferraz Leite, the Director of so many international microsurgical workshops around the world, for his open-minded and valuable teaching culture.

We acknowledge support from the Open Access Publishing Fund of Karl Landsteiner University of Health Sciences, Krems, Austria. This study was funded by a grant from the Scientific Fund of the Mayor of Vienna. The cost of this publication was funded by the Open Access Publishing Fund of Karl Landsteiner University of Health Sciences, Krems,

Austria. The funding bodies played no role in the design of the study, the collection, analysis, and interpretation of the data, and the writing of the manuscript.

## References

1. Molyneux, A. J. et al. International subarachnoid aneurysm trial (ISAT) of neurosurgical clipping versus endovascular coiling in 2143 patients with ruptured intracranial aneurysms: A randomised comparison of effects on survival, dependency, seizures, rebleeding, subgroups, and aneurysm occlusion. *Lancet*. **366** (9488), 809-817 (2005).
2. Algra, A. M. et al. Procedural clinical complications, case-fatality risks, and risk factors in endovascular and neurosurgical treatment of unruptured intracranial aneurysms: A systematic review and meta-analysis. *JAMA Neurology*. **76** (3), 282-293 (2019).
3. Laurent, D. et al. The evolution of endovascular therapy for intracranial aneurysms: Historical perspective and next frontiers. *Neuroscience Insights*. **17**, 26331055221117560 (2022).
4. Böcher-Schwarz, H. G. et al. Histological findings in coil-packed experimental aneurysms 3 months after embolization. *Neurosurgery*. **50** (2), 375-379 (2002).
5. Sherif, C., Plenk, H. J., Grossschmidt, K., Kanz, F., Bavinzski, G. Computer-assisted quantification of occlusion and coil densities on angiographic and histological images of experimental aneurysms. *Neurosurgery*. **58** (3), 559-566 (2006).
6. Massoud, T. F., Guglielmi, G., Ji, C., Viñuela, F., Duckwiler, G. R. Experimental saccular aneurysms. I. Review of surgically-constructed models and their laboratory applications. *Neuroradiology*. **36** (7), 537-546 (1994).
7. Anidjar, S. et al. Elastase-induced experimental aneurysms in rats. *Circulation*. **82** (3), 973-981 (1990).
8. Wakhloo, A. K., Schellhammer, F., de Vries, J., Haberstroh, J., Schumacher, M. Self-expanding and balloon-expandable stents in the treatment of carotid aneurysms: An experimental study in a canine model. *AJNR. American Journal of Neuroradiology*. **15** (3), 493-502 (1994).
9. Dai, D. et al. Histopathologic and immunohistochemical comparison of human, rabbit, and swine aneurysms embolized with platinum coils. *American Journal of Neuroradiology*. **26** (10), 2560-2568 (2005).
10. Shin, Y. S. et al. Creation of four experimental aneurysms with different hemodynamics in one dog. *American Journal of Neuroradiology*. **26** (7), 1764-1767 (2005).
11. Abruzzo, T. et al. Histologic and morphologic comparison of experimental aneurysms with human intracranial aneurysms. *AJNR. American Journal of Neuroradiology*. **19** (7), 1309-1314 (1998).
12. Sherif, C., Plenk, H. J. Quantitative angiographic and histopathologic evaluation of experimental aneurysms. *American Journal of Neuroradiology*. **32** (2), E33 (2011).
13. Sherif, C. et al. Microsurgical venous pouch arterial-bifurcation aneurysms in the rabbit model: Technical aspects. *Journal of Visualized Experiments*. (51), e2718 (2011).
14. Sherif, C. et al. Very large and giant microsurgical bifurcation aneurysms in rabbits: Proof of feasibility and comparability using computational fluid dynamics

- and biomechanical testing. *Journal of Neuroscience Methods*. **268**, 7-13 (2016).
15. Marbacher, S. et al. Long-term patency of complex bilobular, bisaccular, and broad-neck aneurysms in the rabbit microsurgical venous pouch bifurcation model. *Neurological Research*. **34** (6), 538-546 (2012).
  16. Sherif, C., Marbacher, S., Erhardt, S., Fandino, J. Improved microsurgical creation of venous pouch arterial bifurcation aneurysms in rabbits. *American Journal of Neuroradiology*. **32** (1), 165-169 (2011).
  17. Spetzger, U. et al. Microsurgically produced bifurcation aneurysms in a rabbit model for endovascular coil embolization. *Journal of Neurosurgery*. **85** (3), 488-495 (1996).
  18. Bavinzski, G. et al. Experimental bifurcation aneurysm: A model for in vivo evaluation of endovascular techniques. *Minimally invasive neurosurgery*. **41** (3), 129-132 (1998).
  19. Forrest, M. D., O'Reilly, G. V Production of experimental aneurysms at a surgically created arterial bifurcation. *American Journal of Neuroradiology*. **10** (2), 400-402 (1989).
  20. Ysuda, R., Strother, C. M., Aagaard-Kienitz, B., Pulfer, K., Consigny, D. A large and giant bifurcation aneurysm model in canines: proof of feasibility. *American Journal of Neuroradiology*. **33** (3), 507-512 (2012).
  21. Marbacher, S. et al. Complex bilobular, bisaccular, and broad-neck microsurgical aneurysm formation in the rabbit bifurcation model for the study of upcoming endovascular techniques. *American Journal of Neuroradiology*. **32** (4), 772-777 (2011).
  22. Sherif, C., Marbacher, S., Fandino, J. Computerized angiographic evaluation of coil density and occlusion rate in embolized cerebral aneurysms. *Acta Neurochirurgica*. **153** (2), 343-344 (2011).